

## EFFECT OF HEAT TREATMENT IN MAGNETIC PROPERTIES AND MICROSTRUCTURE OF NdFeB-BASED PERMANENT MAGNETS PRODUCED BY STRIP CASTING ALLOYS

Marcela E. M. Faria<sup>1\*</sup>, Suzilene C. Janasi<sup>1</sup>, Suelanny C. Silva<sup>2</sup>, Jorge C. Silva Filho<sup>3</sup>,  
Hidetoshi Takiishi<sup>1</sup>, Luis G. Martinez<sup>1</sup>

1 – Nuclear and Energy Research Institute, IPEN, 05508000, São Paulo, SP

2 – Escola Politécnica of the University of São Paulo, EPUSP, 05508010, São Paulo, SP.

3 - Federal University from ABC, UFABC, 09210-580, Santo André, SP.

[Marcelaenaile@yahoo.com.br](mailto:Marcelaenaile@yahoo.com.br)

### ABSTRACT

*Nd<sub>14</sub>Fe<sub>ba1</sub>B<sub>6</sub> sintered magnets were produced from a strip casting (SC) alloy, obtained on a pilot scale. The SC alloy was submitted to heat treatments (HT) of 2.5 h and 5 h at 1373 K under a vacuum atmosphere and then processed by the powder metallurgy route to obtain the magnets. The SC alloys with and without HT were fragilized in hydrogen (H<sub>2</sub>), milled and, the powders resultants were aligned in a 6 T pulsed field, compacted in an isostatic press at 200 MPa and vacuum sintered at 1373 K during 1 h. The X-ray diffraction results showed the presence of magnetic 2:14:1 phase and Fe in the SC alloy without the HT. After the HT of 2,5 h and 5 h, only 2:14:1 phase was observed, indicating that the HT was sufficient to homogenize the alloy. The microstructural analysis of the alloy after 5 h of HT by scanning electron microscopy (SEM) showed the presence of 2:14:1 phase, confirming the XRD results. The increase in grain size of the alloys after the heat treatment resulted in sintered magnets with larger grains compared with the magnet obtained from the alloy without the heat treatment. The highest magnetic properties among all samples were obtained in magnet produced from the alloy submitted to heat treatment during 5 h, which exhibited the following values  $iH_c = 462 \text{ kAm}^{-1}$  and  $J_r = 1.27 \text{ T}$ .*

**Keywords:** magnetic alloys, microstructure, heat treatment, NdFeB magnets, Dy

### INTRODUCTION

Ternary rare earth magnets have been studied since 1983<sup>1,2</sup>. The Re-Fe-B magnets had shown the highest  $(BH)_{max}$  from all the commercialized magnets<sup>3,4</sup>. As many countries around the world are banning conventional combustion engines, by 2040 they will be replaced by electric ones, thus a great effort is being invested in research to develop better RE-magnets<sup>5</sup>.

Research on permanent magnets with superior properties focuses on compounds with high values of the Curie temperature ( $T_c > 500 \text{ K}$ ) and high values at magnetic properties as remanence ( $J_r$ ), intrinsic coercivity ( $iH_c$ ) and maximum energy product  $(BH)_{max}$ <sup>6,7</sup>. In the RE-Fe-B magnets, the  $T_c$  is low ( $\sim 583 \text{ K}$ )<sup>8,9</sup>, when compared with the other magnets. Magnetite

has a  $T_c$  of  $\sim 856\text{ K}^{10}$ ,  $\text{SmCo}_5$   $\sim 953\text{ K}^{12}$ , Alnico  $\sim 1003\text{ K}^{13}$  and some ferrites have a  $T_c$  around  $738\text{ K}^{14}$ .

One way to improve the  $T_c$  and the other properties is by changing the processing parameters<sup>15</sup> or adding alloy elements, such as: Dy, Ti, Nb<sup>16,17,18</sup>. Takiishi et al, describes some of the factors that directly impact in the magnetic properties of permanent magnets such the milling time to obtain magnetic powders<sup>21</sup>.

## MATERIALS AND METHODS

The commercial strip casting (SC) alloy was obtained from Less Common Metal Ltd (Birkenhead, England). Its composition is  $\text{Nd}_{14}\text{B}_6\text{Fe}_{\text{bal}}$ . After x ray diffraction (XRD) analysis it was verified the presence of  $\alpha\text{-Fe}$ , which is deleterious to the magnetic properties. In order to eliminate the  $\alpha\text{-Fe}$  detected, the alloy was submitted to a heat treatment. The temperature of heat treatment was  $1373\text{ K}$  and two different times were tested  $2.5\text{ h}$  and  $5\text{ h}$ . Then the alloys were submitted again to an XRD analysis and to SEM to confirm that the  $\alpha\text{-Fe}$  was removed.

The process to obtain the magnets began with the hydrogen decrepitation.  $15\text{ g}$  of  $\text{Nd}_{14}\text{B}_6\text{Fe}_{\text{ba}}$  alloy in small pieces ( $< 5\text{ mm}$ ) was placed in a stainless-steel hydrogenation vessel which was evacuated to backing pump.  $\text{H}_2$  was inserted in the vessel with a pressure of  $2\text{ bar}$ , causing the alloy decrepitation. The hydride of the material was milling in a planetary ball mill (*Fritsch Pulverisette*) at  $200\text{ rpm}$ . Stainless steel spheres were used in the ratio (spheres/powder-weight)  $10:1$ , cyclohexane was used to avoid oxidation and samples were milled by  $60\text{ min}$ . The resultant powders were dried and transferred to a rubber tube under inert atmosphere. The powders were pulsed at  $6\text{ T}$  magnetic field, isostatically pressed at  $200\text{ MPa}$  and sintered under vacuum at  $1373\text{ K}$  during  $60\text{ min}$ .

Table 1 correlates the magnets obtained and the duration of the heat treatment used in each one. The L1\_60, was the original one and no HT was applied on it; L1TT2.5\_60 and L1TT5\_60 had  $2.5\text{ H}$  and  $5\text{ H}$  of HT treatment, respectively. These two temperatures were used to check which would be enough to eliminate the free iron and

Table 1: Identification of the produced magnets from the  $\text{Nd}_{14,1}\text{B}_{6,1}\text{Fe}_{\text{bal}}$  alloy and the respective heat treatment time realized in the SC alloy.

Sample	Heat Treatment (h)
L1_60	0
L1TT2.5_60	2.5
L1TT5_60	5

The magnetic characterization was done using a permeameter to obtain the hysteresis loop. The microstructure was observed using a SEM. The crystallography data was obtained with a diffractometer (Rigaku, Ultima IV) with  $\text{Cu-K}\alpha$  radiation. Grain size measurements were analyzed using the software ImageJ.

## RESULTS AND DISCUSSION

In the Figure 1 are shows the X ray diffraction (XRD) results obtained from  $\text{Nd}_{14}\text{B}_6\text{Fe}_{\text{ba}}$  SC alloy. In the diffractogram corresponding to the Nd14 original alloy (without heat treatment)

were identified the magnetic phase  $\text{Nd}_2\text{Fe}_{14}\text{BH}_{1.04}$  (PDF#86-274) and  $\alpha\text{-Fe}$  (PDF#85-1410) which is deleterious to magnetic properties. The presence of  $\alpha\text{-Fe}$  in SC alloys is not expected because the rapid cooling of the alloy during the production process should prevent the growth of dendrites phase of  $\alpha\text{-Fe}$ .

The diffractogram from the Nd14 alloy sample with heat treatment of 2.5 h and 5 h presented just the  $\text{Nd}_2\text{Fe}_{14}\text{BH}_{4.73}$  phase (PDF#86-277), which proves that the HT was effective to remove the free iron, that appeared in alloy without treatment.

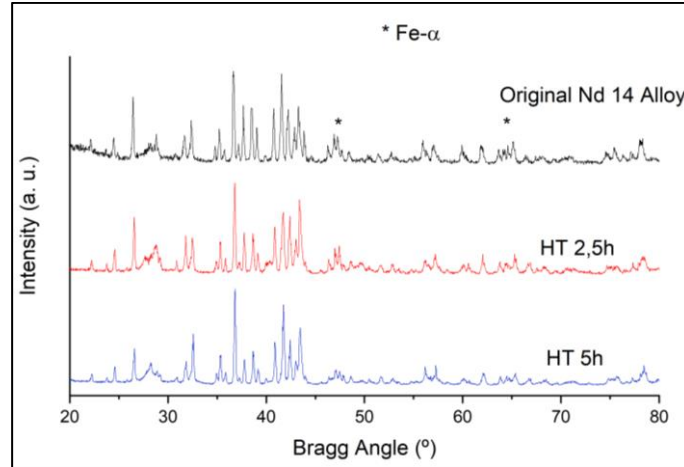


Figure 1: the XRD profile obtained from the Nd14 original alloy, and the alloy with heat treatment of 2.5 h and 5 h at 1373 K.

It is shown in Figure 2 (a-c) the microstructures of the  $\text{Nd}_{14}\text{B}_6\text{Fe}_{ba}$  SC alloy with and without heat treatment.

The sample without the heat treatment (Figure 2 a) presented a lamellar microstructure composed of columnar grains of  $\text{Nd}_2\text{Fe}_{14}\text{B}$  phase (light gray contrast) which is surrounded by the rich-Nd phase uniformly distributed among the grains. It was not possible to identify the  $\alpha\text{-Fe}$  phase by the micrograph.

As expected, with increasing heat treatment time (Figure 2 b - c), a significant increase in grain size was observed. After the heat treatments, the micrographs show refinement of columnar  $\text{Nd}_2\text{Fe}_{14}\text{B}$  grains at equiaxed and rich-Nd phase at triple junctions (white contrast).

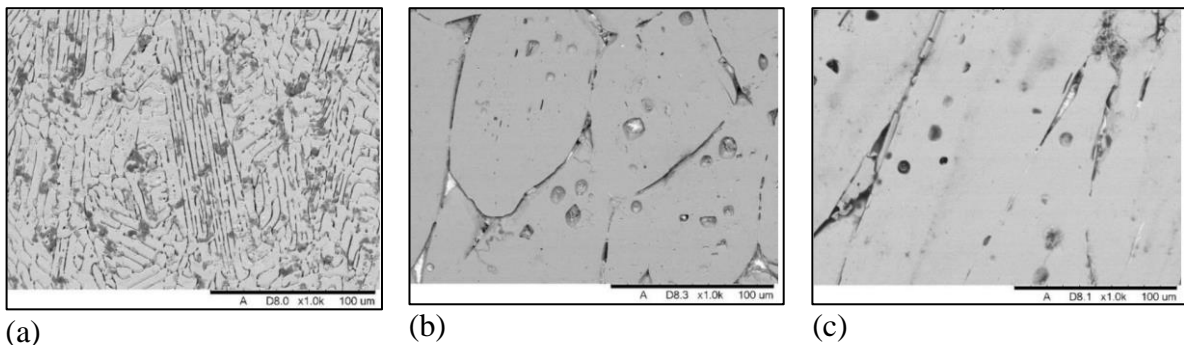


Figure 2:  $\text{Nd}_{14}\text{B}_6\text{Fe}_{bal}$  SC alloy with and without heat treatment, the images were obtained with SEM (a) without heat treatment, (b) heat treated at 1373 during 2.5 h (c) heat treated at 1373 K during 5 h.

Figures 3 (a-b) and 4 (a-b) show the micrographs and histograms of the average grain size distribution from the L1TT2.5\_60 and L1TT5\_60 magnets, respectively. The grain boundaries were revealed after a superficial chemical etched.

The average grain size and the standard deviation were obtained using the software image J, for the magnet L1TT2.5\_60 was  $\bar{d} = (4.57 \pm 3.42)\mu\text{m}$  and for L1TT5\_60 was  $\bar{d} = (5.15 \pm 3.89)\mu\text{m}$ . With an increase of the heat treatment time, the medium grain size also increases. The heterogeneity was confirmed by the high standard deviation values. Even though the widely grain size distribution, most of the grains are below  $10\mu\text{m}$ . The average grain size values of the magnets produced in this work are situated within the range between  $2$  and  $6\mu\text{m}$ , as suggested in previous studies for Nd-Fe-B sinterized magnets<sup>1</sup>. Rodewald et al. (1997) verified that larger grains are deleterious to the coercivity, once the probability of reverse domain nucleation increase according to the grain size.

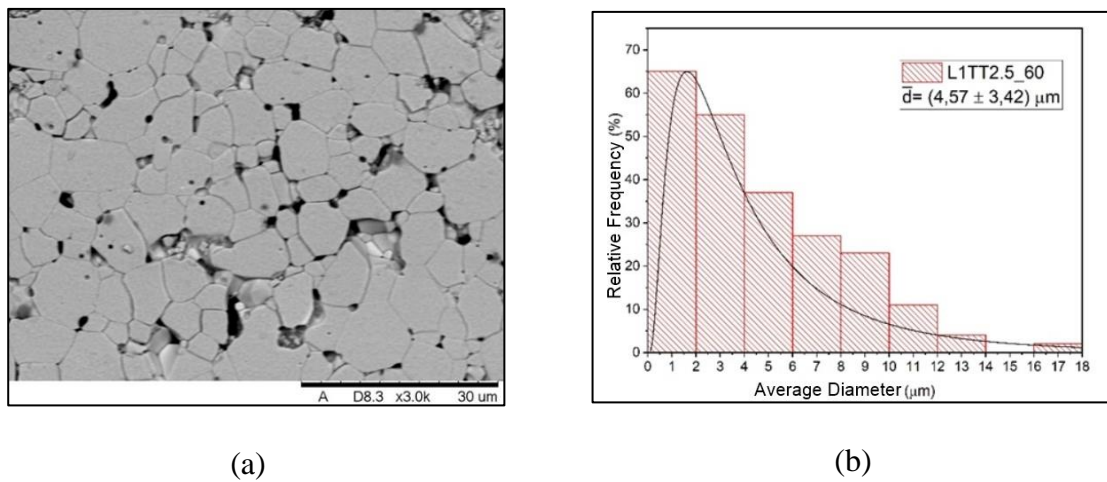


Figure 3: (a) SEM image and (b) Grain size distribution of L1TT2.5\_60 magnet.

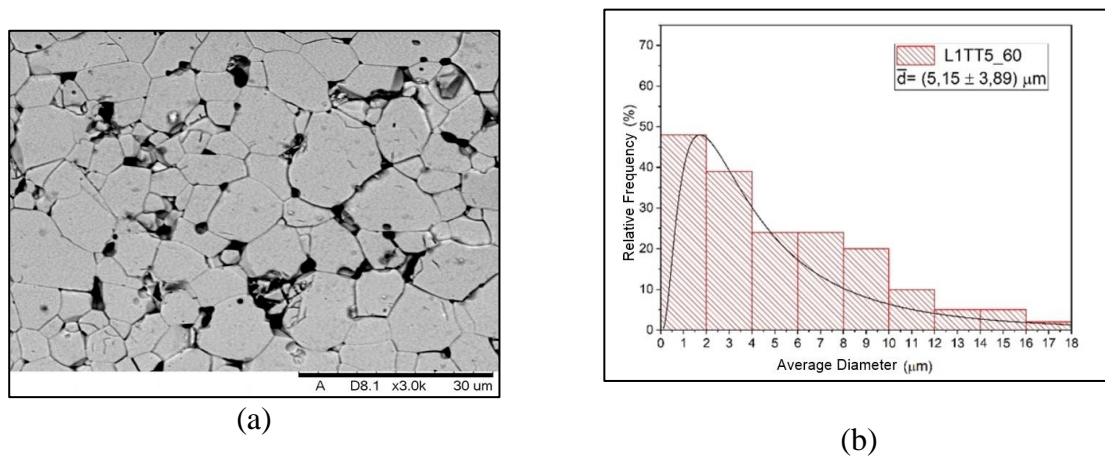


Figure 4: (a) SEM image and (b) Grain size distribution of L1TT5\_60 magnet.

The magnetic properties of magnets produced are shown in Figure 5. Table 2 shows the information summarized. It was verified that the magnet obtained from the  $\text{Nd}_{14}\text{B}_6\text{Fe}_{\text{bal}}$  SC alloy with HT of 5 h resulted in a magnet with better magnetic properties. The grain sizes obtained from the alloy with 5 h of HT also showed the presence of smaller grains than the magnet obtained from 2.5 h of HT. Which results in a high intrinsic coercivity.

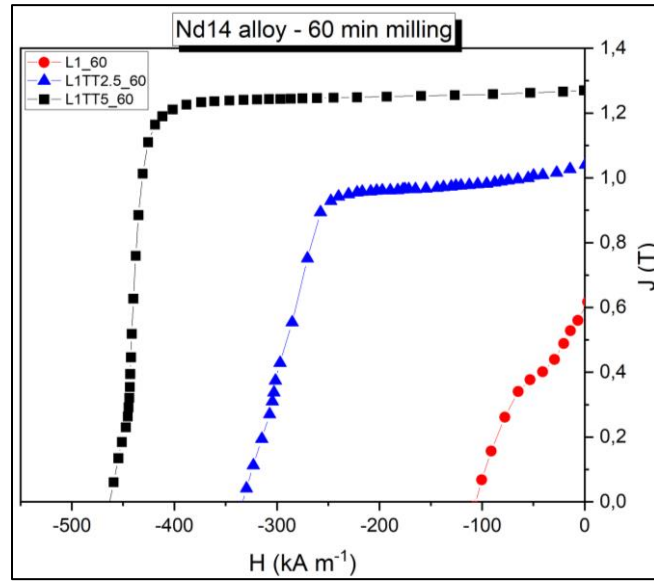


Figure 5: Demagnetization curves of the magnets produced with  $\text{Nd}_{14}\text{B}_6\text{Fe}_{\text{bal}}$  SC alloy without heat treatment and heat treated during 2.5 and 5 h at 1373 K.

Table 2: Summary of magnetic properties of L1\_60, L1TT2.5\_60 and L1TT5\_60 magnets.

Sample	$iH_c$ (kA.m <sup>-1</sup> )	$J_r$ (T)	$BH_{\text{max}}$ (kJ.m <sup>-3</sup> )
L1_60	106.7	0.62	71.5
L1TT2.5_60	358	1.05	154.0
L1TT5_60	462	1.27	287.0

## CONCLUSIONS

Heat treatment was efficient to remove the free iron from the alloys and to homogenize the microstructure, which reflected in better magnetic properties. Although the 2.5 h of heat treatment was enough to eliminate the free iron, the grain size distribution was also more heterogenized when compared with the treated sample for 5 h. The average grain sizes obtained for the L1TT2.5\_60 magnet was (4,47  $\mu\text{m}$ ) and L1T\_60 was (5,15  $\mu\text{m}$ ) are within the range of 2 and 6  $\mu\text{m}$ , as suggested in the literature for the RE sintered magnets. The highest magnetic properties among all the samples were obtained in magnet produced from the alloy submitted to heat treatment during 5 h (L1TT5\_60), and exhibited the following values of  $iH_c = 462 \text{ kAm}^{-1}$  and  $J_r = 1.27 \text{ T}$ .

## ACKNOWLEDGEMENTS

The authors acknowledge Dr. Hidetoshi Takiishi by his scientific support. Marcela Enaile de Melo Faria acknowledge CAPES for the scholarship.

## REFERENCES

1. FIM, R. G. T. Influência dos Parâmetros de Processamento na Microestrutura e nas Propriedades Magnéticas de Ímãs Permanentes de (Nd, Pr)FeB. 2018, 83p. Dissertação (Mestrado em Tecnologia Nuclear – Materiais) - Instituto de Pesquisas Energéticas e Nucleares. IPEN-CNEN/SP, São Paulo.
2. SILVA, M. R. M. Influência de Elementos de Liga na Microestrutura e Propriedades Magnéticas de Ímãs a Base de Pr-Fe-B. 2017, 96p. Dissertação (Mestrado em Tecnologia Nuclear – Materiais) - Instituto de Pesquisas Energéticas e Nucleares. IPEN-CNEN/SP, São Paulo.
3. GUTFLEISCH, O. Controlling the Properties of High Energy Density Permanent Magnetic Materials by Different Processing Routes. *J. Phys. D. Appl. Phys.*, v. 33, p. R157-R172, 2000.
4. VAIMANN, T.; KALLASTE, A.; KILK, A.; BELAHCE, A. Magnetic Properties of Reduced Dy NdFeB Permanent Magnets and Their Usage in Electrical Machines, *IEEE*, p. 1-5, 2013.
5. NAKAMURA, H. The Current and Future Status of Rare Earth Permanent Magnets. *Scripta Materialia*, v. 154, p. 273-276, 2018.
6. CALLISTER, W. D.; RETHISCH, D. G. *Materials Science and Engineering: an introduction*. Ed. Wiley, 8<sup>th</sup> edition, 2012.
7. BAI, G.; GAO, R. W.; SUN, Y.; HAN, G. B.; WANG, B. Study of High Coercivity Sintered NdFeB magnets. *J. Magn. Magn. Mater.*, v. 308, p. 20-23, 2007.
8. YAN, M. N.; WANG, H.; HEI, Y. F.; YANG, L. Y. M.; MACLENNAN, A.; YANG, B. Relating atomic local structures and curie temperature of NdFeB permanent magnets: an X-ray spectroscopic study. *Rare Metals*, v. 37, p. 983-988, 2018.
9. PANDIAN, S.; CHANDRASEKARAN, V.; MARKANDEYULU, G.; IYER, K. J. L.; RAMA RAO, K. V. S. Effect of Al, Cu, Ga, and Nb additions on the magnetic properties and microstructural features of sintered NdFeB. *J. Appl. Phys.*, v. 92, n. 10. P: 6082-6086, 2002.
10. COEY, J. M. D. *Magnetism and Magnetic Materials*. UK, Cambridge University Press, 2010.
11. HARRIS, I. R.; JEWELL, G. W. *Rare-Earth magnets properties, processing, and applications*. Woodhead Publishing Limited, 2012.
12. CAMPOS, M. F.; LANDGRAF, F. J. G.; SAITO, N. H.; ROMETO, S. A.; NEIVA, A. C.; MISSELL, F. P.; DE MORAIS, E.; GAMA, S.; OBRUCHEVA, E. V.; JALNIN, B. V. Chemical composition and coercivity of SmCo<sub>5</sub> magnets. *J. Appl. Phys.*, v. 84, n. 1, p. 368-373, 1998.
13. TENZER, R. K.; KRONENBERG, K. J. Phase Analysis of Alnico V based on Temperature Effects. *Journal of Applied Physics*, v. 29, n. 3, p. 302-303, 1958.
14. FRANCO, A.; SILVA, M. S. High temperature magnetic properties of magnesium ferrite nanoparticles. *J. Appl. Phys.* v. 109, 2011.
15. ZHANG, W. Y.; CHIU, C. H.; ZHANG, L. C.; BISWAS, K.; EHRENBERG, H.; CHANG, W. C. ECKERT, J. Complete suppression of metastable phase and significant enhancement of magnetic properties of B-rich PrFeB nanocomposites prepared by devitrifying amorphous ribbons. *J. Magn. Magn. Mater.*, v. 308, p. 24-27, 2007.
16. CHANG, W. C.; CHIOU, D. Y.; WU, S. H.; MA, B. M.; BOUNDS, C. O. High performance  $\alpha$ -Fe/Nd<sub>2</sub>Fe<sub>14</sub>B-type nanocomposites. *Applied Physics Letter*, v. 121, n.72, p. 121-124, 1998.
17. WANG, J. L.; TANG, N.; SHEN, Y. P.; YANG, D.; FUQUAN, B.; WU, G. H.; YANG, F. M.; DE BOER, F. R.; BRÜCK, E.; BUSCHOW, K. H. J. Structural and magnetic properties of R(Fe<sub>1-y</sub>Co<sub>y</sub>)<sub>12-x</sub>Nb<sub>x</sub> compounds. *J. Appl. Phys.*, v. 91, p. 2165-2171, 2001.
18. MISHRA, R. K.; CHEN, J. K.; THOMAS, G. Effect of annealing on the microstructure of sintered Nd-Fe-B magnets. *J. Appl. Phys.*, v. 59, 1986.
19. KOBAYASHI, K.; URUSHIBATA, K.; UNE, Y.; SAGAWA, M. The origin of coercivity enhancement in newly prepared high coercivity Dy-free Nd-Fe-B sintered magnets. *J. Appl. Phys.*, v. 113, 2013.
20. ZHOU, Q.; LI, W.; HONG, Y.; ZHAO, L.; ZHONG, X.; YU, H.; HUANG, L.; LIU, Z. Microstructure improvement related coercivity enhancement for sintered NdFeB magnets after optimized additional heat treatment. *Journal of Rare Earths*, v.36, p. 379-384, 2018.
21. TAKIISHI, H.; LIMA, L. F. C. P.; COSTA, I.; FARIA, R. N. The influence of process parameters and alloy structure on the magnetic properties of NdDyFeBNb HD sintered magnets. *Journal of Materials Processing Technology*, v. 152, p. 1-8, 2004.
22. RODEWALD, W.; WALL, B.; FERNENGEL, W. Grain Growth Kinetics in Sintered Nd-Fe-B Magnets. *IEEE Trans. Magn.*, v. 33, p. 3841-3843, 1997.